Journal of Power Sources 209 (2012) 251–256

Contents lists available at SciVerse ScienceDirect

Journal of Power Sources

journal homepage: www.elsevier.com/locate/jpowsour

Short communication

Synthesis and electrochemical performance of $Li_3V_2(PO_4)_{3-x}Cl_x$/C cathode materials for lithium-ion batteries

Ji Yan[a,*], Wei Yuan[a], Zhi-Yuan Tang[a], Hui Xie[b], Wen-Feng Mao[a], Li Ma[c]

[a] Department of Applied Chemistry, School of Chemical and Engineering Tianjin University, Tianjin 300072, PR China
[b] Texas Materials Institute, ETC 9.184, University of Texas at Austin, Austin, TX 78712, United States
[c] McNair Technology Co., Ltd., Dongguan, Guangdong 523700, PR China

ARTICLE INFO

Article history:
Received 19 October 2011
Received in revised form 11 January 2012
Accepted 28 February 2012
Available online 9 March 2012

Keywords:
Lithium vanadium phosphate
Chlorine doping
High-rate stability
Cathode
Li ion batteries

ABSTRACT

The Cl-doping $Li_3V_2(PO_4)_3$/C (LVP/C) cathode materials were synthesized by a sol–gel method. The effects of Cl-doping amount on electrochemical properties, structure and morphology of $Li_3V_2(PO_4)_3$/C were studied by electrochemical impedance spectroscopy, cyclic voltammetry, X-ray diffraction, FTIR spectrum and scanning electron microscopy. The results indicate that the $Li_3V_2(PO_4)_{2.88}Cl_{0.12}$/C composite presents an excellent discharge capacity as high as 106.95 mAh g^{-1} after 80 cycles at 8 C. The same monoclinic structure of $Li_3V_2(PO_4)_{2.88}Cl_{0.12}$/C sample can be obtained from XRD analysis while the particle size is smaller than that of pristine sample ($x = 0$). The FTIR results further confirm the substitution of Cl^- for PO_4^{3-}. The reasons for the relatively enhanced capability are attributed to the decreased polarization and the reduced charge transfer resistance of electrode, with the suitable Cl-doping amount of $x = 0.12$.

1. Introduction

Lithium ion batteries are considered to be the most promising rechargeable batteries for PHEV (plug-in hybrid electric vehicle) and the electric energy storage for solar and wind energy sources [1]. Cathode material plays a critical role in determining the power density and safety of battery. Recently, lithiated metal phosphates $LiFePO_4$ [2] and $Li_3V_2(PO_4)_3$ [3–7] have drawn much attention from world-wide researchers due to their outstanding safety merits. Compared to the well-known phosphate ($LiFePO_4$ (LFP)), monoclinic $Li_3V_2(PO_4)_3$ (LVP) exhibits even higher discharge capacity, better Li-ion diffusion efficiency and higher energy density (530 Wh kg^{-1}) [8]. In LVP, all three lithium ions can be reversibly extracted from the lattice sites with a theoretical capacity as high as 197 mAh g^{-1}, and the 3D rigid framework with distorted VO_6 octahedra and PO_4 tetrahedra sharing corner with each other benefits LVP to achieve an exceptional ionic conductivity [9]. However, the pristine LVP also faces to the intrinsic low electronic conductivity as LFP, which largely limits its rate performance.

Up to now, several techniques have been carried out to increase the electronic conductivity of LVP: (i) coating various carbon materials [10,11]; (ii) mixing other high electron conductive metal particles [12,13] and (iii) reducing the particle size to nano size [14]. On the other hand, doping a slight amount of other alien ions has been widely used as another effective method to enhance the electron conductivity of LVP, such as Al^{3+} [15], Mg^{2+} [16] and Co^{2+} [17]. Partial substitution of anion (F^- ion at the PO_4^{3-} site) [18] has also been reported because that the substitution of F^- for PO_4^{3-} can improve the cycling stability and the tap density of LVP through catalyzing the particle growth.

In this work, we firstly report the effect of Cl-doping on the discharge capacity and high-rate capacity retention of LVP. The influence of Cl-doping on the structural, micro-morphology and electrochemical performance of LVP material is also discussed in detail.

2. Experimental

The $Li_3V_2(PO_4)_{3-x}Cl_x$/C ($x = 0$, 0.04, 0.08, 0.12 and 0.16) composites were synthesized by a sol–gel method. Stoichiometric amounts of Li_2CO_3, V_2O_5, $NH_4H_2PO_4$ and NH_4Cl (to yield 0.01 mol $Li_3V_2(PO_4)_{3-x}Cl_x$) were dissolved into critic acid solution (2.83 g in 150 ml demonized water) by violently stirring at room temperature. Then, the pH of the solution was adjusted to about 9 by adding $NH_3{\cdot}H_2O$ drop-wise with continuous stirring for 3 h until a green transparent sol formed. The excess water of the sol was evaporated at 80 °C and the obtained gel was heated at 120 °C and then pre-calcined at 350 °C for 4 h to release NH_3 and H_2O under N_2 atmosphere. The precursor was ground, pelletized and calcined

* Corresponding author. Tel.: +86 769 8301 7180; fax: +86 769 8319 5372.
E-mail address: jiyan@tju.edu.cn (J. Yan).

0378-7753/$ – see front matter © 2012 Elsevier B.V. All rights reserved.
doi:10.1016/j.jpowsour.2012.02.110

at 850 °C for 8 h under the same atmosphere. The residual carbon amount of final product was about 6.5% [19], which was obtained by dissolving the powders in hydrochloric acid and the remaining was weighted.

The phase purity and structural analysis of the as-synthesized samples were performed by powder X-ray diffraction (XRD, Bruker D8 diffractometer) using Cu-Kα radiation. The morphology and microstructure of as-synthesized composites were observed with filed emission scanning electron microscopy (FESEM, Tecnai G2 F20).

The electrochemical performances of the $Li_3V_2(PO_4)_{3-x}Cl_x/C$ (x = 0, 0.04, 0.08, 0.12 and 0.16) samples were investigated by assembling 2032 type coin cells. The cathode electrodes were fabricated by blending the as-prepared active powder with super P and PTFE (60% in ethanol) in a weight ratio of 80:10:10. The loading density of the materials almost reached 2.4 mg cm^{-2}. The coin cells were assembled in an argon-filled glove box to avoid contamination by air and moisture, using one of the synthesized materials as cathode, lithium metal as anode and 1 M $LiPF_6$ in EC/DMC (1:1, by volume ratio) as electrolyte. Galvanostatically charge and discharge tests were performed utilizing a battery tester (NEWARE, BTS-610) between 3.0 and 4.3 V at room temperature. The cyclic voltammetry tests were operated between 3.0 and 4.5 V at a scanning rate of 0.1 mV s^{-1}. Electrochemical impedance spectroscopy tests were conducted on a Gamry electrochemical workstation (No. PCI 4-750) with frequency range from 0.1 Hz to 10 kHz and the potential amplitude of 5 mV.

3. Results and discussion

The initial charge–discharge curves of the $Li_3V_2(PO_4)_{3-x}Cl_x/C$ (x = 0, 0.04, 0.08, 0.12 and 0.16) samples at 0.2 C (1 C = 133 mAh g^{-1}) rate are compared in Fig. 1a. It is shown that with the increase of Cl^- amount, the specific discharge capacities of the materials present an enhanced trend and the highest value of 127.32 mAh g^{-1} is obtained for x = 0.12. Compared with the profile of pristine LVP/C, the charge–discharge plateau of $Li_3V_2(PO_4)_{2.88}Cl_{0.12}/C$ is a little longer and the sloping plateau of $Li_3V_2(PO_4)_{2.88}Cl_{0.12}/C$ may attribute to the inductive effect of the stronger electronegative Cl^- ion [20,21]. The substitution of stronger electronegative Cl^- for PO_4^{3-} may decrease the Li—O bond energy and leads to an easily extraction of lithium ion, which will change the solid solution range of $Li_3V_2(PO_4)_3$. This change can be expressed from the change of the equilibrium concentration of Li-deficient and Li-rich phases, evidencing from the equilibrium potential curves [20]. It is believed that the substitution of PO_4^{3-} with Cl^- does not disturb the electrochemical behavior and structure stability of LVP/C largely [22]. Moreover, the cycle performances of $Li_3V_2(PO_4)_{3-x}Cl_x/C$ (x = 0, 0.04, 0.08, 0.12 and 0.16) at 0.5 C are given in Fig. 1b. For x = 0.04, the discharge capacity of the sample is not improved significantly compared with un-doped one, while its capacity retention is slightly decreased. An improved discharge capacity is found for x = 0.08. For x = 0.12, the discharge capacity reaches the highest value among various samples at 0.5 C, its discharge capacity reaches 123.79 mAh g^{-1} and only fades to 122.15 mAh g^{-1} (98.7%) after 50 cycles. The observed increased capacity retention may be attributed to the enhanced electron conductivity and the improved Li^+ diffusion ability after Cl-doping [22]. Obviously, the $Li_3V_2(PO_4)_{2.88}Cl_{0.12}/C$ sample presents the highest discharge capacity and good cycling performance.

Electrochemical impedance spectra measurements of the samples are also carried out under the state of inactivation. The corresponding Nyquist plots are shown in Fig. 2a. All the impedance spectra consists a semicircle at high frequency and a linear tail at low frequency. The semicircle at high frequency region is attributed

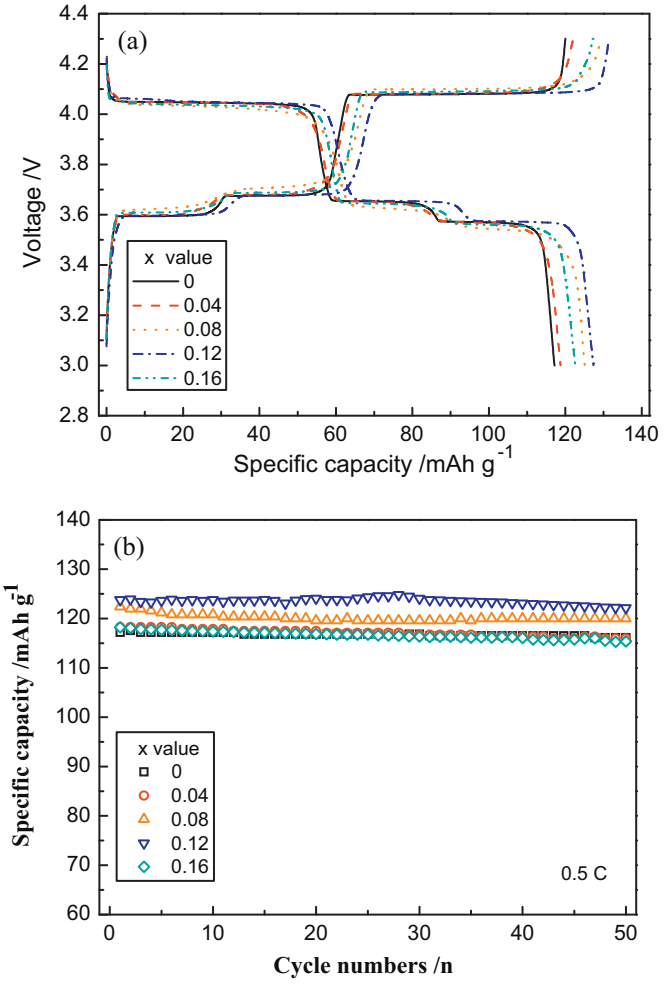

Fig. 1. (a) The initial charge–discharge curves of the $Li_3V_2(PO_4)_{3-x}Cl_x/C$ (x = 0.00, 0.04, 0.08, 0.12 and 0.16) at 0.2 C rate. (b) The cycle performances of the composites at 0.5 C rate.

to the charge transfer resistance (R_{ct}) [23], and the sloping line in low frequency is attributed to the lithium ion diffusion in solid phase. As shown in Fig. 2a, with the doping amount of Cl^- ion increasing from 0 to 0.16, the R_{ct} representing for an overlapped depressed semicircle from the R_{ct} at the $Li_3V_2(PO_4)_3$/electrolyte and at the lithium metal/electrolyte interface almost maintains the same value with the un-doped sample and then decreases sharply, and the minimum value is obtained at x = 0.12 [24]. One possible reason is that partial substitution of PO_4^{3-} with Cl^- in LVP stimulates the electrochemical activation of lithium ion, which can be well illuminated by the increased discharge capacity and the decreased charge transfer resistance. Generally, the electron conductivity and lithium ion diffusion rate are two key factors in controlling the high-rate performance of LVP/C. The lithium ion diffusion coefficient is calculated based on the following equation [25]:

$$D = \frac{R^2T^2}{2A^2n^4F^4C^2\sigma^2}$$

where R is the gas constant, T the absolute temperature, A the surface area of the cathode, n the number of electrons per molecule during oxidization, F the Faraday constant, C the concentration of lithium-ion (herein, 2.216×10^{-2} mol cm^{-3}), and σ is the Warburg factor which is associated with the Z_{re}.

$$Z_{re} = R_s + R_{ct} + \sigma\varpi^{-1/2}$$

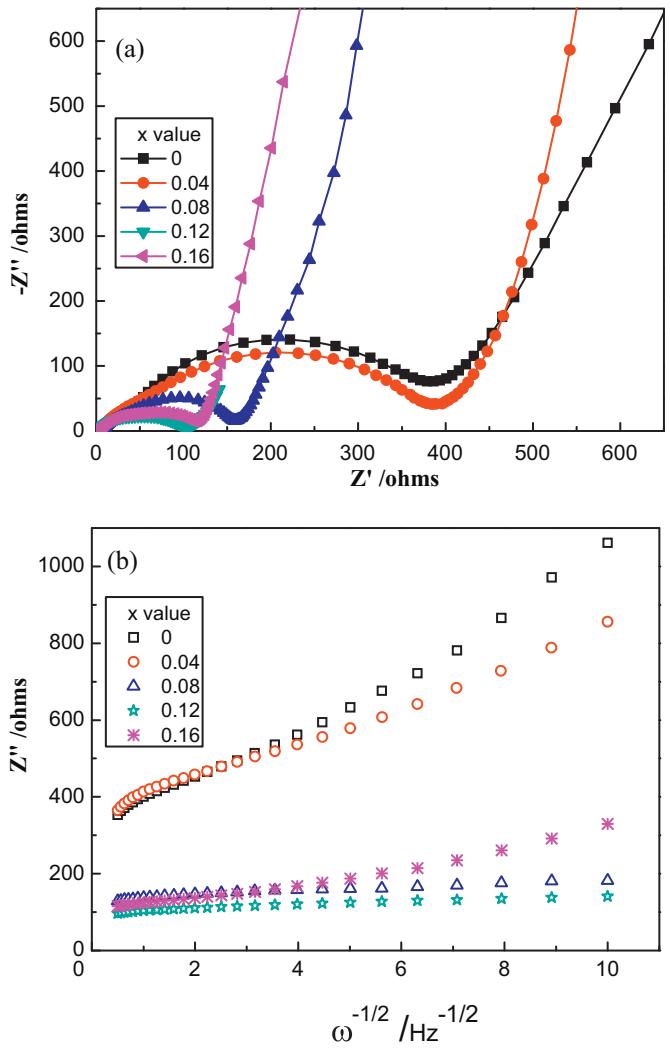

Fig. 2. (a) Electrochemical impedance spectra of the $Li_3V_2(PO_4)_{3-x}Cl_x/C$ ($x = 0.00$, 0.04, 0.08, 0.12 and 0.16) and (b) the relationship plot between Z_{re} and $\omega^{-1/2}$ at low-frequency region.

where R_s is the resistance of interface film resistance and R_{ct} the charge transfer resistance.

The calculated lithium ion diffusion coefficients of $Li_3V_2(PO_4)_{3-x}Cl_x/C$ ($x = 0$, 0.04, 0.08, 0.12 and 0.16) at inactivate state are 2.55×10^{-12}, 5.43×10^{-12}, 4.04×10^{-10}, 5.78×10^{-10} and 2.94×10^{-11} $cm^2\,s^{-1}$, respectively. The D_{Li^+} value increases with x and reaches the maximum at $x = 0.12$. Based on above analysis, $Li_3V_2(PO_4)_{2.88}Cl_{0.12}/C$ is considered as the optimal doping sample.

As shown in Fig. 3, the discharge capacities of the pristine LVP/C and $Li_3V_2(PO_4)_{2.88}Cl_{0.12}/C$ diverge obviously at the higher rates (above 5 C), and the higher capacity retention is detected for the $Li_3V_2(PO_4)_{2.88}Cl_{0.12}/C$. A capacity of 113.58 mAh g^{-1} is obtained after 80 cycles at 5 C rate with a capacity retention of 90.27%. In comparison, the pristine LVP/C only delivers a capacity of 105.11 mAh g^{-1} after 80 cycles. When the rate is up to 8 C, the capacities of the pristine LVP/C and $Li_3V_2(PO_4)_{2.88}Cl_{0.12}/C$ after 80 cycles are found to be 90.55 and 106.95 mAh g^{-1}, respectively. The 10th charge–discharge curves of $Li_3V_2(PO_4)_{2.88}Cl_{0.12}/C$ at 5 C and 8 C is given in the inset of Fig. 3. A slight polarization between the charge–discharge plateaus of $Li_3V_2(PO_4)_{2.88}Cl_{0.12}/C$ with the increasing rate is observed, which is attributed to the reduced polarization and faster lithium ion diffusion rate.

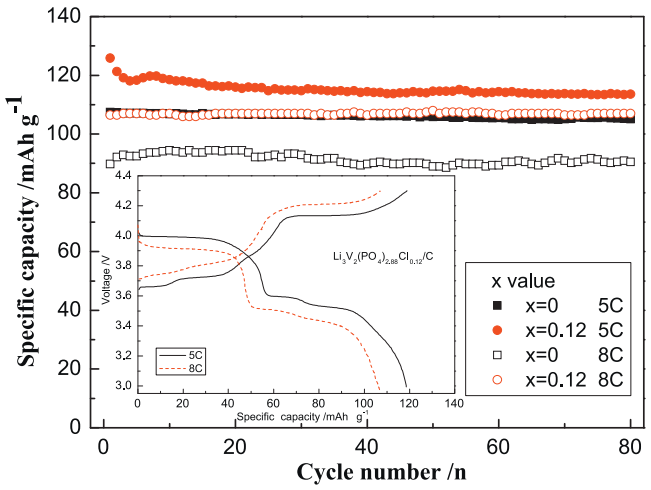

Fig. 3. The cycling performance of the pristine LVP/C and $Li_3V_2(PO_4)_{2.88}Cl_{0.12}/C$ at the high rates of 5 C and 8 C (inset is the 10th charge–discharge profiles of $Li_3V_2(PO_4)_{2.88}Cl_{0.12}/C$ at 5 C and 8 C).

The CV curves of the pristine LVP/C and $Li_3V_2(PO_4)_{2.88}Cl_{0.12}/C$ are shown in Fig. 4. It is shown that the improved electrochemical reversibility of LVP/C is attributed to the enhanced electronic conductivity resulting from the rearrangement of electric cloud of P—O after Cl-doping, as previous report by F-doping [26]. Three pairs of clear separated peaks represent two redox reactions from $Li_3V_2(PO_4)_3$, $Li_2V_2(PO_4)_3$ to $LiV_2(PO_4)_3$. Furthermore, after the Cl-doping, the anodic peaks shift toward higher potential and the cathodic peaks shift toward lower potential, indicating that the polarization between each redox has been alleviated and the extraction and insertion process of lithium ions become easier. As reported by Sun et al. [22], the introduction of Cl element can improve the electrochemical kinetics of LVP/C. This also correlates with the excellent electrochemical performance under the high charge–discharge rates. The mechanisms for the pristine sample ($x = 0$) and Cl = 0.12 sample are given in below:

$$Li_3V_2^{3+}(PO_4)_3 \underset{\text{Insertion}}{\overset{\text{Extraction}}{\rightleftarrows}} LiV_2^{4+}(PO_4)_3 + 2Li^+ + 2e^-$$

$$Li_3V_2^{3+}(PO_4)_{2.88}Cl_{0.12} \underset{\text{Insertion}}{\overset{\text{Extraction}}{\rightleftarrows}} LiV^{3+}V^{4+}(PO_4)_{2.88}Cl_{0.12} + 2Li^+ + 2e^-$$

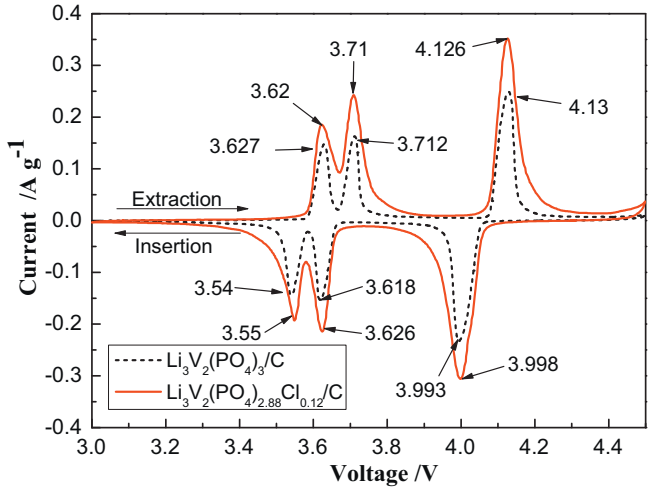

Fig. 4. CV curves of the pristine LVP/C and $Li_3V_2(PO_4)_{2.88}Cl_{0.12}/C$ with a scanning rate of 0.1 mV s^{-1} in the range of 3.0–4.5 V.

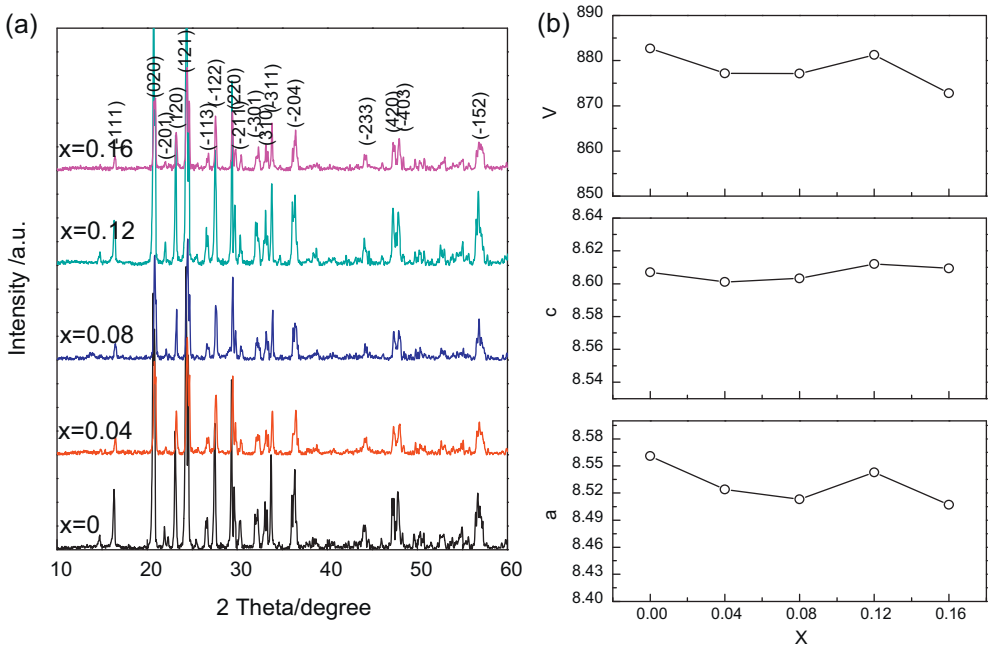

Fig. 5. XRD patterns of the pristine LVP/C and $Li_3V_2(PO_4)_{2.88}Cl_{0.12}$/C.

Herein, the Cl-doping induces the formation of mixing valence V^{3+}/V^{4+} and more easy extraction of lithium ion from the lattice sites, which facilitate for reducing the phase boundary of $Li_3V_2(PO_4)_3$ and improve the capability performance. The change from multi-phase reaction to single-phase reaction could effectively affect the phase-boundary and results in improved lithium ion diffusion coefficient and good electrochemical performance [27].

The XRD patterns for pristine LVP/C and Cl-doping samples are shown in Fig. 5a. We notice that the obtained Cl-doping samples are well crystallized and have no difference from the pristine LVP/C. The obtained Cl-doping composites maintain monoclinic structure with space group $P2_1/n$, demonstrating that Cl^- ion has dissolved into the crystal structure of LVP. No impurity is detected from the XRD patterns. The effects of Cl-doping amount on the lattice parameters of *a*, *b* and *c* are also studied. From Table 1 and Fig. 5b, we notice that the parameter of *a* delivers a shrunken trend with the increase of Cl-doping amount, while the parameters of *b* and *c* do not exhibit any rule. The results cannot satisfy the Vegard's Law because of the low content substitution of Cl^- [28]. In addition, no peaks of crystal carbon can be seen from the patterns indicating that the surface coating carbon is amorphous structure and does not affect the structure of LVP.

In order to further confirm the substitution of Cl^- for PO_4^{3-}, we tested the FTIR spectrum and the results are shown in Fig. 6. It has been proven that the FTIR spectrum can be used to study the local environment of cations in the lattice of close-packed oxygen atoms because of the sensitivity of vibration modes of cations [29]. Herein, we also use the FTIR spectrum to confirm the substitution of Cl doping for PO_4^{3-}. The fundamental stretching vibrational frequency of tetrahedral PO_4^{3-} ion is in the range of 1600–1300 cm^{-1}. From Fig. 6, a peak at 1649.25 cm^{-1} is detected for the $Li_3V_2(PO_4)_{2.88}Cl_{0.12}$/C, while the pristine $Li_3V_2(PO_4)_3$/C has a peak at 1596.82 cm^{-1}, attributing to PO_4^{3-} (γ_1). The red shift of peak indicates that Cl^- has been doped into the matrix of $Li_3V_2(PO_4)_3$ and results in an inductive effect in lattice. The results consist with the XRD analysis. In addition, the introduction of Cl^- may cause the rearrangement of electronic cloud in PO_4^{3-} polyion and increases the conductivity [30].

Fig. 7 shows the SEM images of the obtained pristine LVP/C and $Li_3V_2(PO_4)_{2.88}Cl_{0.12}$/C. It can be seen that both samples are uniform in the surface morphology. From the observation of the particle size, the dominant size of the pristine is about 2–3 μm. However, the smaller particles in the range of about 1 μm appear in the $Li_3V_2(PO_4)_{2.88}Cl_{0.12}$/C. It is well known that the large specific

Table 1
Lattice parameters of the pristine LVP/C and $Li_3V_2(PO_4)_{2.88}Cl_{0.12}$/C.

Samples	*a* (Å)	*b* (Å)	*c* (Å)	*V* (Å^3)
Pristine LVP/C	8.561	11.978	8.607	882.71
$Li_3V_2(PO_4)_{2.96}Cl_{0.04}$/C	8.524	11.964	8.6011	877.19
$Li_3V_2(PO_4)_{2.92}Cl_{0.08}$/C	8.513	11.975	8.6033	877.13
$Li_3V_2(PO_4)_{2.88}Cl_{0.12}$/C	8.543	11.975	8.612	881.24
$Li_3V_2(PO_4)_{2.84}Cl_{0.16}$/C	8.507	11.916	8.6093	872.80

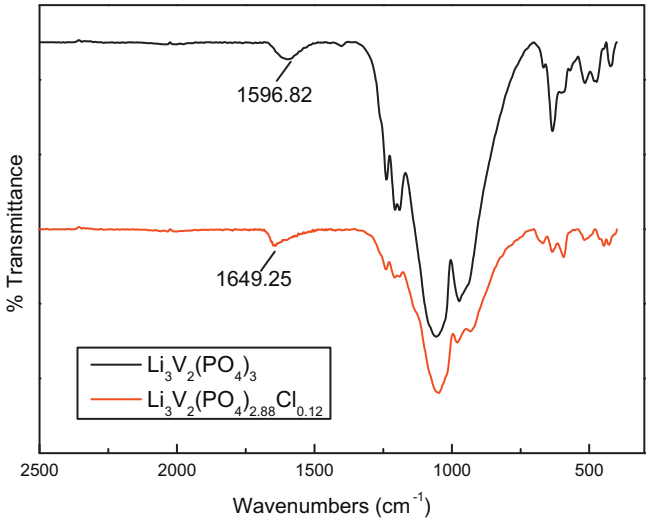

Fig. 6. FTIR spectrum of LVP/C and $Li_3V_2(PO_4)_{2.88}Cl_{0.12}$/C.

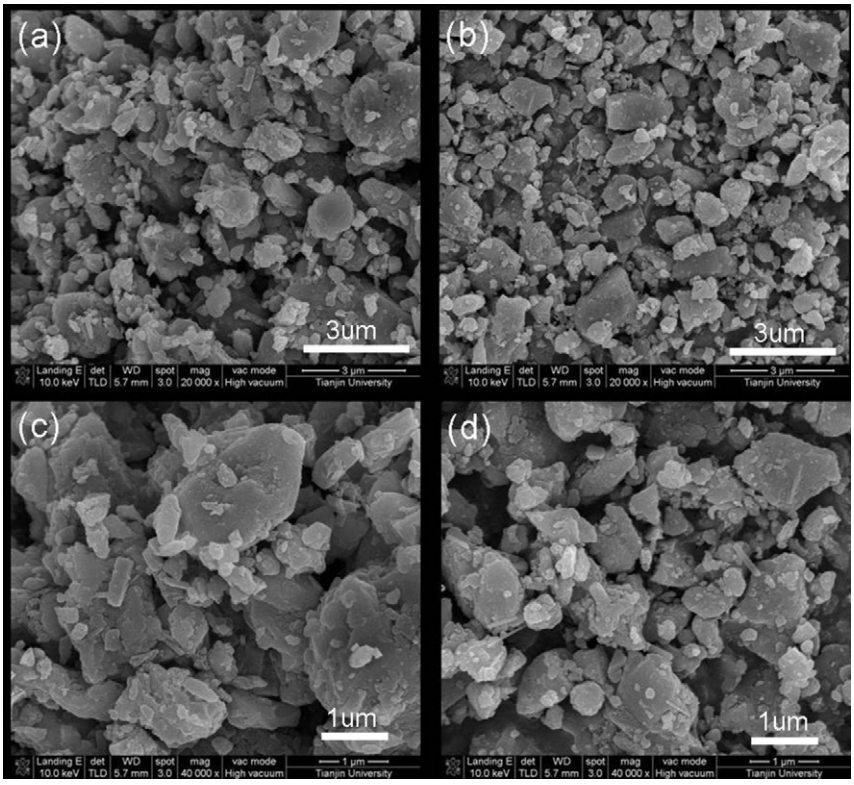

Fig. 7. SEM images of the pristine LVP/C (a) and (c), and $Li_3V_2(PO_4)_{2.88}Cl_{0.12}$/C (b) and (d).

surface area and uniform particle size would be very effective in enhancing the high-rate capability of the material [31]. The uniform particle distribution can increase the contacted area between the electrolyte and electrode, which may favor the electrolyte penetration. The smaller particle decreases the lithium ion diffusion distance that is beneficial for high-rate performance. In this work, our experimental results suggest that the good electrochemical rate performance can be benefited from the smaller particle size and better structure stability at a moderate Cl-doping content.

4. Conclusion

In this work, Cl-doping $Li_3V_2(PO_4)_3$/C cathode materials were firstly prepared by a sol–gel method. The results show that the doping increases the discharge capacities of $Li_3V_2(PO_4)_3$/C, and the highest value is obtained for doping amount of Cl = 0.12. The high rate capabilities at 5 C and 8 C rates are also improved significantly by doping. The phenomena can be explained from the improved stability of structure and the ameliorated polarization of electrode after Cl-doping. The well introduction of Cl^- ion into the crystal of $Li_3V_2(PO_4)_3$/C and the reduced particle size after Cl-doping are preferable for the high-rate capability and cycling performance of $Li_3V_2(PO_4)_3$/C.

Acknowledgments

This study was supported by National Science Foundation of China (Grant No. 20973124) and Guangdong Sci. & Tech. Key Projects (Grant No. 2009A080208001). In addition, the authors wish to thank Dr. Tong-huan Yang for the XRD analysis.

References

[1] H. Li, Z. Wang, L. Chen, X. Huang, Advanced Materials 21 (2009) 4593–4607.
[2] A.K. Padhi, K.S. Nanjundaswamy, J.B. Goodenough, Journal of the Electrochemical Society 144 (1997) 1188–1194.
[3] Y.N. Ko, H.Y. Koo, J.H. Kim, J.H. Yi, Y.C. Kang, J.-H. Lee, Journal of Power Sources 196 (2011) 6682–6687.
[4] K. Nagamine, T. Honma, T. Komatsu, Journal of Power Sources 196 (2011) 9618–9624.
[5] A. Pan, D. Choi, J.-G. Zhang, S. Liang, G. Cao, Z. Nie, B.W. Arey, J. Liu, Journal of Power Sources 196 (2011) 3646–3649.
[6] Y.Q. Qiao, X.L. Wang, Y.J. Mai, J.Y. Xiang, D. Zhang, C.D. Gu, J.P. Tu, Journal of Power Sources 196 (2011) 8706–8709.
[7] L.-L. Zhang, Y. Li, G. Peng, Z.-H. Wang, J. Ma, W.-X. Zhang, X.-L. Hu, Y.-H. Huang, Journal of Alloys and Compounds 513 (2012) 414–419.
[8] C. Dai, Z. Chen, H. Jin, X. Hu, Journal of Power Sources 195 (2010) 5775–5779.
[9] M.Y. Saıdi, J. Barker, H. Huang, J.L. Swoyer, G. Adamson, Electrochemical Solid-State Letters 5 (2002) A149–A151.
[10] Y.Q. Qiao, J.P. Tu, Y.J. Mai, L.J. Cheng, X.L. Wang, C.D. Gu, Journal of Alloys and Compounds 509 (2011) 7181–7185.
[11] H. Liu, P. Gao, J. Fang, G. Yang, Chemical Communications 47 (2011) 9110–9112.
[12] T. Jiang, Y.J. Wei, W.C. Pan, Z. Li, X. Ming, G. Chen, C.Z. Wang, Journal of Alloys and Compounds 488 (2009) L26–L29.
[13] L. Zhang, X.L. Wang, J.Y. Xiang, Y. Zhou, S.J. Shi, J.P. Tu, Journal of Power Sources 195 (2010) 5057–5061.
[14] A. Pan, J. Liu, J.-G. Zhang, W. Xu, G. Cao, Z. Nie, B.W. Arey, S. Liang, Electrochemistry Communications 12 (2010) 1674–1677.
[15] D. Ai, K. Liu, Z. Lu, M. Zou, D. Zeng, J. Ma, Electrochimica Acta 56 (2011) 2823–2827.
[16] J.S. Huang, L. Yang, K.Y. Liu, Y.F. Tang, Journal of Power Sources 195 (2010) 5013–5018.
[17] Q. Kuang, Y. Zhao, X. An, J. Liu, Y. Dong, L. Chen, Electrochimica Acta 55 (2010) 1575–1581.
[18] S. Zhong, L. Liu, J. Liu, J. Wang, J. Yang, Solid State Communications 149 (2009) 1679–1683.
[19] P. Fu, Y. Zhao, Y. Dong, X. An, G. Shen, Journal of Power Sources 162 (2006) 651–657.
[20] U.S. Kasavajjula, C. Wang, P.E. Arce, Journal of the Electrochemical Society 155 (2008) A866–A874.
[21] J.B. Goodenough, Y. Kim, Chemistry of Materials 22 (2010) 587–603.
[22] C.S. Sun, Y. Zhang, X.J. Zhang, Z. Zhou, Journal of Power Sources 195 (2010) 3680–3683.
[23] F. Gao, Z. Tang, Electrochimica Acta 53 (2008) 5071–5075.
[24] D. Zane, Electrochimica Acta 49 (2004) 4259–4271.
[25] B. Jin, E.M. Jin, K.-H. Park, H.-B. Gu, Electrochemistry Communications 10 (2008) 1537–1540.

[26] L. Yang, L. Jiao, Y. Miao, H. Yuan, Journal of Solid State Electrochemistry 14 (2009) 1001–1005.
[27] S. Liu, S. Li, K. Huang, Z. Chen, Acta Physico-Chimica Sinica 23 (2007) 537–542.
[28] M. Kageyama, D. Li, K. Kobayakawa, Y. Sato, Y.-S. Lee, Journal of Power Sources 157 (2006) 494–500.
[29] A. Rougier, G.A. Nazri, C. Julien, Ionics 3 (1997) 170–176.
[30] L. Yang, L. Jiao, Y. Miao, H. Yuan, Journal of Solid State Electrochemistry 13 (2008) 1541–1544.
[31] Q. Kuang, Y. Zhao, Z. Liang, Journal of Power Sources 196 (2011) 10169–10175.